ACS APPLIED MATERIALS & INTERFACES

Research Article

www.acsami.org

Improving the Performance of Light-Emitting Electrochemical Cells by Optical Design

Nikolai Kaihovirta, Christian Larsen, and Ludvig Edman*

The Organic Photonics and Electronics Group, Department of Physics, Umeå University, SE-901 87 Umeå, Sweden

ABSTRACT: The organic light-emitting electrochemical cell (LEC) has emerged as an enabling technology for a wide range of novel and low-cost emissive applications, but its efficiency is still relatively modest. The focus in the field has so far almost exclusively been directed toward limiting internal loss mechanisms, whereas external losses resulting from poor light-outcoupling have been overlooked. Here, we report a straightforward procedure for improving the efficiency and emission quality of LECs. We find that our high-performance glass-encapsulated LECs exhibit a near-ideal Lambertian emission profile but that total internal reflection at the glass/air interface and a concomitant edge emission and self-absorption represent a significant loss factor. We demonstrate a 60% improvement in the outcoupled luminance in the forward direction by laminating a light-outcoupling film, featuring a hexagonal array of hemispherical microlenses as the surface structure, onto the front side of the device and a large-area metallic reflector onto the back side. With this scalable approach, yellow-emitting LEC devices with a power conversion efficiency of more than 15 lm W^{-1} at a luminance of 100 cd m^{-2} were realized. Importantly, we find that the same procedure also can mitigate problems with spatial variation in the light-emission intensity, which is a common and undesired feature of large-area LECs.

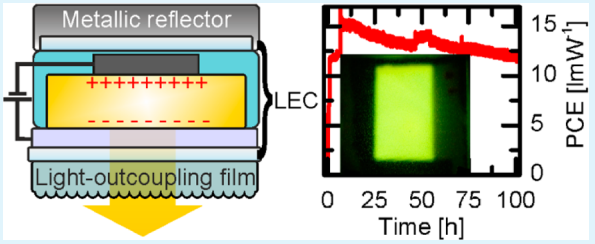

KEYWORDS: *light-emitting electrochemical cell, microlens array, light outcoupling, conjugated polymer, power conversion efficiency, Super Yellow*

1. INTRODUCTION

The organic light-emitting electrochemical cell (LEC) is an area-emitting device that can send out diffuse light from conformable, thin, and large-area surfaces. In its simplest manifestation, the LEC comprises an active-material blend of an electroluminescent compound and an electrolyte sandwiched between two coplanar charge-injecting electrodes: one is transparent to allow the light to escape from the device, whereas the other is typically reflective to guide the light in the forward direction of the viewer.[1−7] The LEC shares the appearance and several operational features with another area-emitting device, the organic light-emitting diode (OLED), but is distinguished from the OLED by its unique fit for low-cost and scalable fabrication. In fact, it has recently been demonstrated that functional LEC devices can be fabricated in a roll-to-roll compatible manner under uninterrupted ambient conditions akin to how newspapers and magazines are produced;[8−11] in contrast, today's commercial high-performance OLEDs are fabricated in clean rooms using expensive high-vacuum processes.

However, although the performance of LECs indeed has been improved markedly as of late, it is still lagging behind the OLED. The important power conversion (or wall-plug) efficiency (PCE) of state-of-the-art OLEDs now exceeds 100 lm W^{-1},[12−15] whereas the corresponding current champion values are almost 40 lm W^{-1} for triplet-emitting small-molecule LECs[16,17] and ∼10 lm W^{-1} for singlet-emitting polymer LECs.[18−20] In this context, it is notable that the high efficiency of OLEDs is the result of a long-term systematic work aimed towards limiting both the internal losses (resulting from nonoptimized charge-injection balance, charge recombination, photoluminescence yield, etc.)[12,21−31] and external losses (resulting from poor light-outcoupling),[12,13,32−45] whereas to date, the focus in the LEC field almost exclusively has been directed toward limiting the former losses.[5,18,20,46−52] Because the external losses can amount to very high values in this type of optical structures, comprising emission from an optically thick active material to a viewer positioned in an optically thin medium (i.e., air), it is now timely to take a closer look into how the light-outcoupling of LECs can be improved.

Here, we show that our high-performance glass-encapsulated LECs exhibit a near-ideal Lambertian emission profile but that the external light-outcoupling at the glass/air interface represents a significant loss factor. By laminating a light-outcoupling film (LOF), with a surface structure in the form of a hexagonal array of hemispherical microlenses, onto the front glass of the device and attaching a large-area metallic reflector onto the back glass, we were able to attain an improvement in the efficiency by a factor of 1.6 during long-term measurements. Specifically, we report a record-high PCE of 15.6 lm W^{-1} at a luminance of 100 cd m^{-2} from a polymer LEC. Moreover, as the LOF randomizes the directions of the light rays emanating

Received: December 3, 2013
Accepted: January 27, 2014
Published: January 27, 2014

   dx.doi.org/10.1021/am405530d | ACS Appl. Mater. Interfaces 2014, 6, 2940−2947

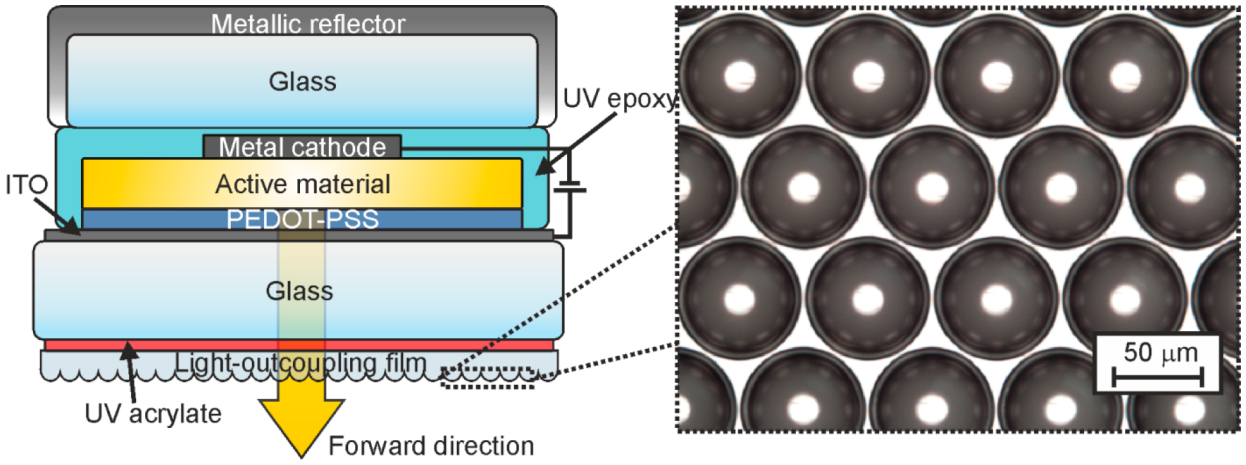

Figure 1. Schematic structure of the glass-encapsulated LEC device with a LOF attached on the front side and a metallic reflector attached on the back side. The right-hand image displays a micrograph of the LOF, showing the hexagonal array of microlenses.

from the device surface, we also report a distinct quantitative improvement in the spatial emission homogeneity from large-area LECs following the inclusion of the LOF.

2. MATERIALS AND METHODS

The first part of the LEC fabrication followed a previously established protocol.[46] A glass substrate (d = 0.7 mm, Eagle XG) coated with a 145 nm thick layer of indium–tin oxide (ITO, Thin Film Devices Inc.) was cleaned by sequential ultrasonication in acetone and isopropanol and afterwards was dried in an oven at T = 120 °C for >12 h. A 40 nm thick layer of PEDOT-PSS was spin-coated onto the clean ITO surface from a water dispersion (Clevios P VP AI 4083, Heraeus GmbH) under ambient air. The sample was thereafter dried at T = 120 °C for >6 h before being transferred into a N_2-filled glove box ([O_2], [H_2O] < 1 ppm) for further processing.

The active material comprised a blend of the electroluminescent phenyl-substituted poly(para phenylene vinylene) copolymer (Super Yellow, Merck GmbH), the salt KCF_3SO_3 (Aldrich), and the ion-dissolving and ion-transporting polymer poly(ethylene oxide) (PEO, M_w = 5 × 10^6 g mol^{-1}, Aldrich). The constituent materials were separately dissolved in cyclohexanone (Aldrich) in a 7 g L^{-1} concentration (Super Yellow) and in a 10 g L^{-1} concentration (KCF_3SO_3 and PEO) before being blended together. For the small-area LECs with an emission area of 1.5 × 8.5 mm^2, a Super Yellow/PEO/KCF_3SO_3 mass ratio of 1:0.085:0.03 was used because it allows for small device-to-device variation and good performance.[46] For the large-area LECs with an emission area of 7.0 × 10.5 mm^2, the mass ratio was 1:0.4:0.1, with the higher electrolyte concentration being selected in order to allow for a more fault-tolerant fabrication procedure.[8] The blend solution was spin-coated on top of the PEDOT-PSS and thereafter was dried on a hot plate at T = 70 °C for >6 h. The active-material thickness was d = 85 nm for the small-area LECs and d = 230 nm for the large-area LECs, as measured with a stylus profilometer (Dektak XT, Bruker). An Al electrode was thermally evaporated (at P < 2 × 10^{-6} mbar) on top of the active material using a shadow mask to define the size of the electrode and the light-emission area. For the attainment of peak-efficient devices, ITO/PEDOT-PSS/{Super Yellow:trimethylolpropane ethoxylate:-$LiCF_3SO_3$}/Al LECs were fabricated according to a previously published procedure.[18] The small-area LECs were encapsulated by attaching a glass slide onto the device structure using a UV-curable single-component epoxy adhesive (Ossila). The UV curing was executed with a high-power-density LED (EXFO Omnicure LX400, λ_{peak} = 365 nm, power density = 8 W cm^{-2}). More details on the encapsulation procedure have been reported elsewhere.[53]

The LOF comprised hemispherical lenses in a hexagonal pattern produced on the surface of a 250 μm thick poly(methyl methacrylate) (PMMA) film (Microsharp Corp. Ltd.) (Figure 1). The radius and the height of the microlenses were 35 and 24.5 μm, respectively. A UV-curable and single-component acrylic adhesive (Microsharp Corp. Ltd.) was used for laminating the LOF onto the LEC. Both the LOF and the adhesive feature a refractive index (n) of n = 1.5, which matches that of the glass substrate. Roughly 1 drop of adhesive was applied to the back side of the LOF before it was firmly pressed to the glass-substrate surface of the LEC. The adhesive was thereafter immediately cured via a 30 s exposure from a UV lamp (Spectroline, λ_{peak} = 365 nm, power density = 530 mW cm^{-2}). The lamination of the LOF was carried out in the glove box. The metallic reflector was an 81 μm thick Al foil (1170 Tape, 3M), and it was laminated onto the encapsulation glass with an acrylic adhesive. The complete LEC device structure is depicted in Figure 1.

The small-area LECs were driven and monitored at constant current density (j) using a computer-controlled source-measure unit (Agilent 2722A). The luminance was measured with a calibrated photodiode equipped with an eye-response filter (Hamamatsu Photonics). The photographs were captured with a Canon EOS 500D camera and recorded with identical camera settings under dark conditions.

For the emission-profile characterization, the LEC was mounted on a rotation stage (ThorLabs XYR 1/M), and the device edges were painted with a black marker pen to prevent edge emission from interfering with the large-angle measurements. The luminous intensity was recorded with a photodiode equipped with an eye-response filter (Hamamatsu Photonics) and measured in steps of 10°. During this measurement, the LECs were driven at j = 11.5 mA cm^{-2} using an Agilent E3631A dc power supply.

For the emission-quality studies on large-area LECs, the devices were driven at V = 3.6 V in the glove box. The photographs were captured with a Canon EOS 500D camera under identical camera settings and dark conditions. The 3D plots were plotted in MATLAB software by first converting the photographs to grayscale. The grayscale photographs exhibit a pixel size of 11 × 11 μm^2, and the intensity from each pixel is given by $i_{x,y}$.

3. RESULTS AND DISCUSSION

Figure 2a presents the measured luminous intensity of a LEC with blackened edges (red solid circles) and the theoretical cosine law (black dotted line) as a function of viewing angle in the polar coordinate system. A light emission that obeys the cosine law is the characteristic of a so-called Lambertian emitter, which by definition features the same luminance irrespective of the viewing angle in the forward direction. An inspection of the graph reveals a good agreement between the measured and theoretical data, although the measured luminous intensity slightly exceeds the cosine law at angles around ±45°.

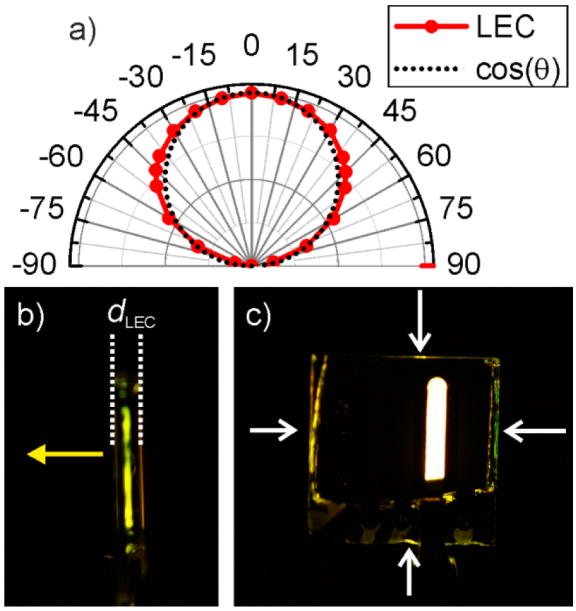

Figure 2. (a) Measured LEC luminous intensity as a function of angle (red solid circles) and the theoretical cosinus function from a Lambertian emitter (black dotted line) presented in polar coordinates. (b) Side-view photograph of the LEC. The yellow arrow indicates the forward direction for light emission. (c) Front-view photograph of the LEC. The white arrows indicate the edge emission originating from the substrate edges. Note that the edges of the LEC in panel a were blackened to eliminate the effects of edge emission.

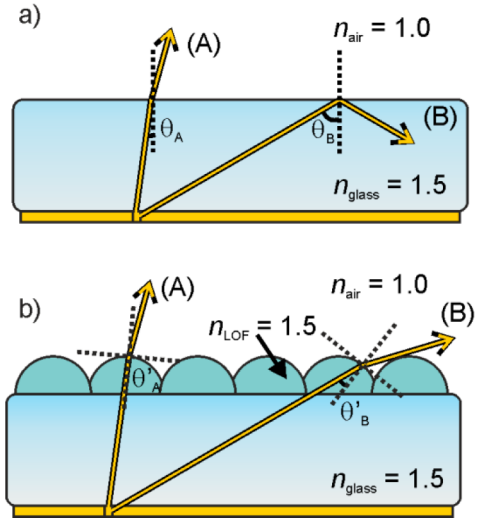

Figure 3. (a) External light-outcoupling at a flat glass/air interface with (A) depicting an outcoupled light beam with $\theta_A < \theta_{TIR}$ and (B) depicting a totally reflected light beam with $\theta_B > \theta_{TIR}$. (b) External light-outcoupling at a glass/air interface with an attached LOF with matching refractive index, for which both light beams (A) and (B) are outcoupled.

Thus, it is appropriate to conclude that this type of LEC device is a near-ideal Lambertian emitter.

An often employed and practical method of calculating the important PCE of LECs (and OLEDs) involves measuring the luminance in the normal direction (at an angle of 0°) and dividing this value with the current density to obtain the current efficacy. The current efficacy is then translated into the PCE by multiplying with π and dividing with the drive voltage.

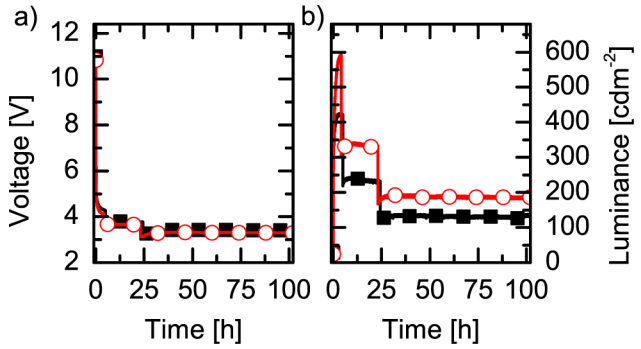

Figure 4. (a) Driving voltage and (b) luminance as a function of time for an LEC with (red open circles) and without (black solid squares) attached LOF. The two steps in device performance correspond to a lowering of the driving current density from an initial value of 15.4 to 7.7 mA cm^{-2} and from 7.7 mA cm^{-2} to the final value of 3.8 mA cm^{-2}.

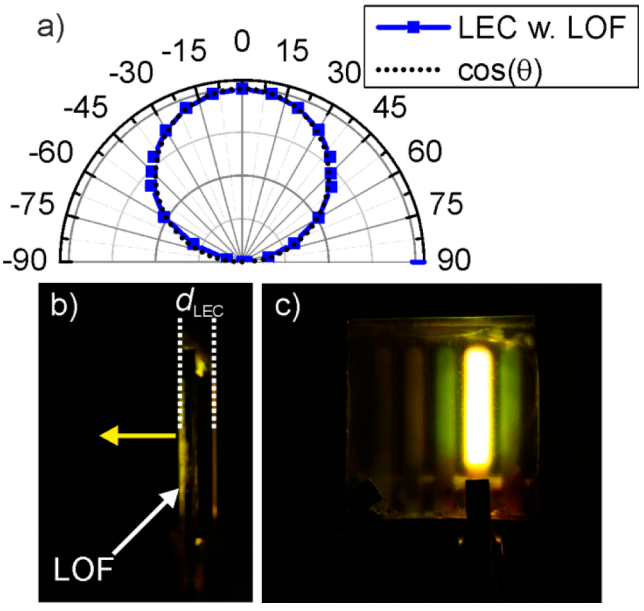

Figure 5. (a) Measured luminous intensity of an LEC with attached LOF as a function of angle (blue solid squares) and the theoretical cosinus function from a Lambertian emitter (black dotted line) presented in polar coordinates. (b) Side-view photograph of an LOF-attached LEC. The yellow arrow indicates the forward direction for light emission. (c) Front-view photograph of the LOF-attached LEC. Note that the edges of the LEC in panel a were blackened to eliminate the effects of edge emission.

It is notable that this procedure of multiplying with π to obtain the PCE value is valid only if the device is an ideal Lambertian emitter.[54] Our above finding thus yields support for this procedure for this particular category of LEC devices. More specifically, as a more detailed analysis of the results in Figure 2a demonstrates that the integral of the measured luminous intensity exceeds the integral of the cosine law by 2.7% (when the 0° value is normalized to be equal for both sets of data), the consequence is that a Lambertian assumption leads to an underestimation of the true PCE for these devices value by the same 2.7%.

Figure 2b and 2c present photographs of the light emission from LEC devices with nonblackened edges probed in the tangential (edge) and normal (forward) directions, respectively. We call attention to fact that significant emission is leaking out

dx.doi.org/10.1021/am405530d | ACS Appl. Mater. Interfaces 2014, 6, 2940−2947

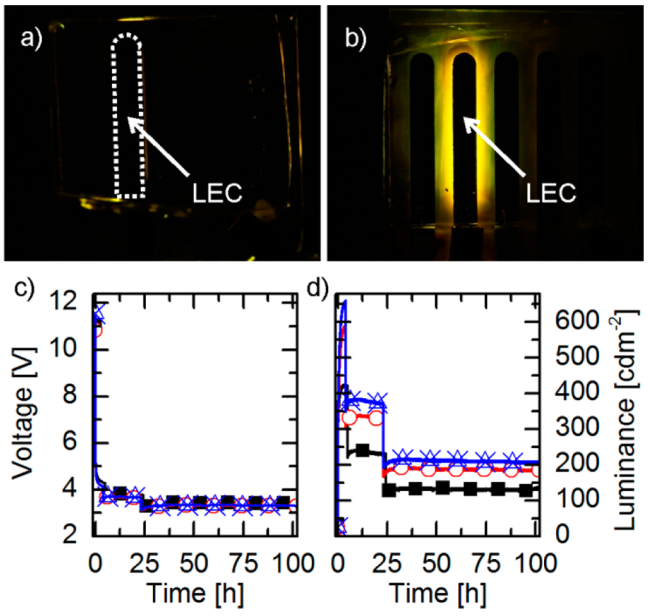

Figure 6. Back-side photographs during light-emission of (a) a bare LEC and (b) an LEC with a LOF attached on the front side. The device contours, as defined by the Al cathode, are indicated by the white dotted line in panel a. (c) Voltage and (d) luminance as a function of time during galvanostatic driving of a bare LEC (black solid squares), an LOF-attached LEC (red open circles), and an LEC with a LOF attached on the front side and a metallic reflector attached on the back side (blue crossed triangles). The two steps in device performance result from a lowering of the driving current density from an initial value of 15.4 to 7.7 mA cm^{-2} and from 7.7 mA cm^{-2} to the final value of 3.8 mA cm^{-2}.

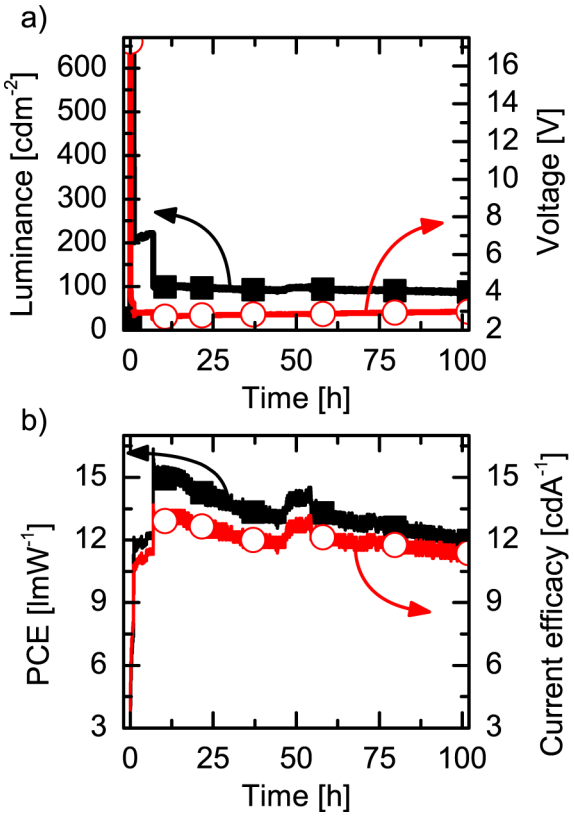

Figure 7. Temporal evolution of (a) luminance (black solid squares) and voltage (red open circles) as well as (b) PCE (black solid squares) and current efficacy (red open circles) for ITO/PEDOT-PSS/{Super Yellow:Trimethylolpropane ethoxylate:LiCF$_3$SO$_3$}/Al LECs with an included LOF and metallic reflector. The LEC is driven in galvanostatic mode, and the driving current density is adjusted in two steps: first from 7.7 to 1.9 mA cm^{-2} and thereafter to the final value of 0.8 mA cm^{-2}.

from the edges of the device, as directly observed in Figure 2b and as indicated by the white arrows in Figure 2c. Such edge emission represents a loss factor for the majority of applications where it is solely the forward emission that is of interest. Moreover, light directed in the edge direction in surface-emitting devices is strongly affected by self-absorption effects, as the optical path length the light has to traverse before exiting the device structure at the edge is much longer than in the forward direction. Thus, it is relevant to quantify the amount of edge-directed light and to develop procedures for limiting this detrimental effect.

A typical LEC device structure comprises a number of optically distinct interfaces, and the edge-directed light originates from when the light ray passes from a medium 1 of higher refractive index to a medium 2 with lower refractive index ($n_1 > n_2$). In such a scenario, total internal reflection (TIR) of a light ray will take place when it hits the interface with an angle of incidence versus the interface normal above the critical angle (θ_c), as dictated by the following modification of Snells law

$$\theta_{TIR} \geq \theta_c = \arcsin(n_2/n_1) \quad (1)$$

The light that is incident on the interface at angles below θ_c thus defines a light-escape cone. For our LEC devices, the light created in the p−n junction is passing (at least) four different interfaces before being emitted (or outcoupled) into the ambient air in the forward direction (Figure 1): (i) active material (AM)/PEDOT-PSS, (ii) PEDOT-PSS/ITO, (iii) ITO/glass, and (iv) glass/air. Measured or estimated values for the refractive index of the constituent materials are available in the literature: n_{AM} (λ = 550 nm) = 1.9,[55] $n_{PEDOT-PSS}$ = 1.5,[56] n_{ITO} = 1.9,[57] n_{glass} = 1.5,[58] and n_{air} = 1.0. An inspection of this particular optical structure reveals that TIR will occur at the AM/PEDOT-PSS interface (i) and the glass/air interface (iv). The TIR-light can be waveguided within the denser optical medium (e.g., the active material or the glass substrate) and either be outcoupled at the edges of the device in the form of edge emission or be subjected to internal self-absorption.

By neglecting optical interference effects and Fresnel reflections and assuming an isotropic light emission in the p−n junction, the fraction of outcoupled light can be calculated with the following equation[59]

$$\eta = 1/(2n_{AM})^2 \quad (2)$$

By plugging in the value for the active-material refraction index, we find that the outcoupling efficiency for our LEC device structure is a mere 14%. This poor total outcoupling efficiency can be divided into an internal outcoupling loss at the AM/PEDOT-PSS interface and an external outcoupling loss at the glass/air interface. Our focus here will be on better understanding and improving the external outcoupling of LEC devices.

To this end, we have investigated the effects of attaching a LOF, in the form of a surface-patterned poly(methyl methacrylate) (PMMA) film, onto the front-glass surface of our LEC devices, as schematically shown in Figure 1. The

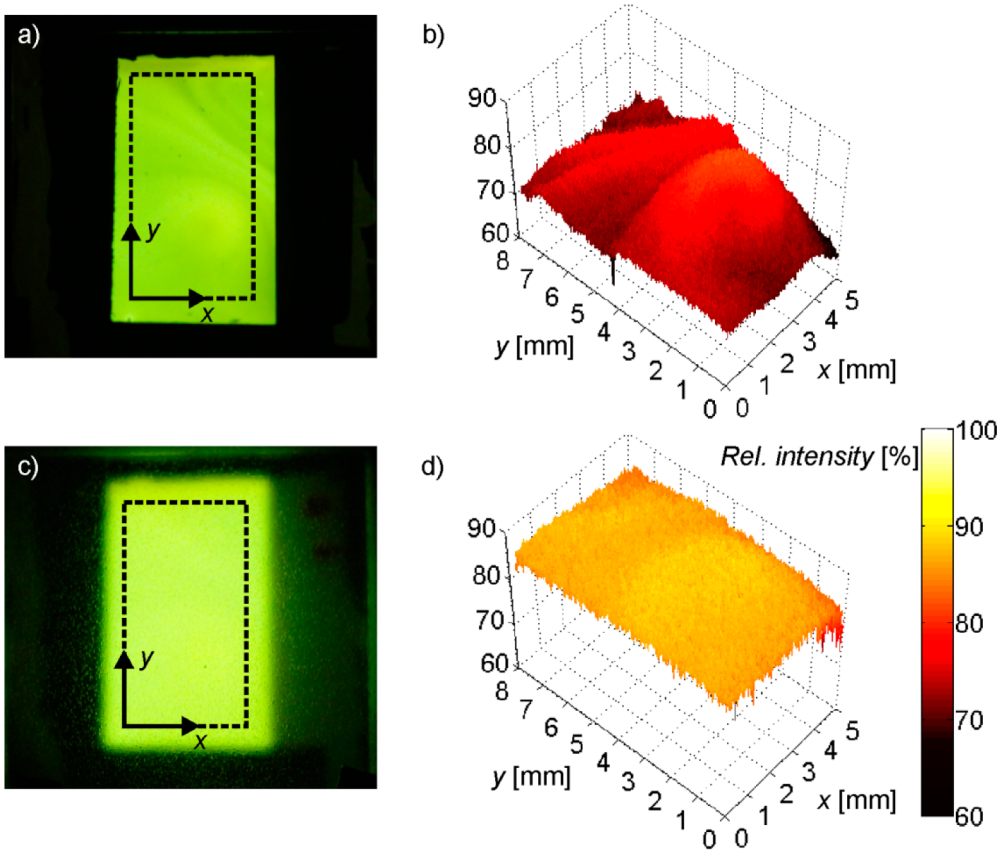

Figure 8. (a) Photograph of a bare large-area LEC. (b) Three-dimensional plot depicting the spatial variation in light intensity of the bare LEC. (c) Photograph of the same LEC as in panel a but with a LOF attached onto the front-glass surface. (d) Three-dimensional plot depicting the spatial variation in light intensity of the LOF-attached LEC. The presented regions in panels b and d are identified by the corresponding dashed outline in panels a and c.

surface pattern of the LOF featured a hexagonal array of hemispherical microlenses, with a radius of 35 μm and a height of 24.5 μm, as depicted in the optical micrograph in Figure 1. This LOF was glued to the front-side glass substrate using an acrylic adhesive, and it is notable that both the adhesive and the PMMA film featured the same refractive index (n = 1.5) as the glass substrate. In other words, no refraction or reflection of light will take place at the glass/LOF interface.

Equation 1 yields that light rays will exhibit TIR when they impinge on a flat glass/air interface with an angle of incidence larger than the critical angle for total reflection: $\theta_{TIR} \geq \theta_{c,air\text{-}glass} = 42°$. Figure 3a shows the two alternative scenarios: (A) a light ray that is outcoupled within the light-escape cone (i.e., $\theta_A < 42°$) and (B) a light ray that is reflected (i.e., $\theta_B > 42°$). However, if the glass/air interface is transformed from being flat to structured via the inclusion of the LOF, then it is possible that light rays with $\theta > \theta_{c,air\text{-}glass}$ also can be outcoupled, as schematically depicted in Figure 3b. However, it is important to point out that the light ray traces depicted in Figure 3a,b were selected to show the positive effect of the LOF, but many light rays still will experience TIR at the glass/air interface. In fact, although a portion of the light rays outside the well-defined flat-glass/air escape cone ($\theta < \theta_{c,air\text{-}glass}$) will be outcoupled by the LOF (as shown in Figure 3b), this will take place at the cost of reduced light-outcoupling within the light-escape cone. We will return to the implications of this fact later in this article.

Nevertheless, a comparative experimental study proves that the inclusion of the LOF actually results in a distinct improvement of the device performance. Figure 4a,b presents the temporal evolution of the voltage and luminance, respectively, during galvanostatic driving of ITO/PEDOT-PSS/{Super Yellow:PEO:KCF_3SO_3}/Al LECs with (red open circles) and without (black solid squares) included LOF. The voltage is, as expected, unaffected by the inclusion of the LOF. The luminance, and as a direct consequence the efficiency, is, in contrast, drastically improved by ~40 % throughout the entire measurement period of 100 h. We point out that this improvement in performance is the calculated average from >10 independent measurements that all display the same generic trend of improved luminance at retained voltage.

It is also of interest to establish the effects of the LOF on the emission properties of the LEC. Figure 5a presents the luminous intensity as a function of viewing angle for the LOF-attached LEC. Similar to the bare LEC data presented in Figure 2a, we find evidence for a near-perfect Lambertian emission for the LOF-attached LEC. A detailed analysis reveals that the Lambertian assumption (see discussion in the context of Figure 2) leads to an underestimation of the true PCE value by a mere 0.3%. We further investigated the influence of the LOF on the electroluminescence (EL) spectrum and find a negligible red shift of the EL peak from 551 to 553 nm and a minor narrowing of the full width at half maximum from 104 to 97 nm (data not shown). Thus, it is clear that the LOF redirects the light without introducing any substantial microcavity or other undesired parasitic optical effects.[32]

More distinct changes are, however, visible in photographs of operating devices. Figure 5b displays the edge emission of the LOF-LEC, and a comparison with the corresponding photograph of the bare LEC in Figure 2b shows that the edge emission is distinctly decreased. (In this context, we call attention to the fact that all photographs throughout the article were recorded with the same camera settings and using the same current density for driving the devices.) This was an anticipated result because an increased outcoupling of light in the forward direction will take place at the expense of the wave-guided modes and the concomitant edge emission.

Figure 5c displays the front-side emission of the LOF-LEC, and the blurry edges of the light emission are striking, particularly in comparison to the sharp edges observed in the front-side emission from the bare LEC in Figure 2c. This LOF-induced effect originates from the combination of two effects: (i) the microlenses in the LOF surface randomizes the directions of the transmitted and reflected light rays at the LOF/air interface and (ii) the employment of a thick glass substrate spreads out the reflected and thereafter transmitted light rays. More specifically, this combination of features allows for new air-outcoupled light rays in the surface-normal direction (that is detected by the camera), which appear to emerge from a point outside of the actual emitting area; thus, the edge blurring results. We note that this this effect is in agreement with previous observations on similar optical systems and that it can be effectively suppressed by the utilization of a thinner substrate.[32,34,35] We also emphasize that although edge blurring indeed is a concern for high-resolution display applications this is not a field of applications for which the LEC technology is particularly fit because of a comparatively slow turn-on time.

Another consequence of the randomization of the directions of the light rays at the LOF/air interface is that a portion of the back-reflected light will not be wave-guided and in addition will miss the reflective cathode so that it can be coupled out on the glass-encapsulated backside of the device. Such an effect is specific to the LOF-attached LEC, as the well-defined TIR light in the bare LEC invariably will be wave-guided in the optical thicker media and will either be coupled out as edge emission or be absorbed within the device structure. Photographs of the back side of a bare LEC and a LOF-attached LEC during light emission are presented in Figure 6a,b, respectively; in agreement with the above argument, we observed a distinct back-side light emission from the LOF-attached LEC but not the bare LEC.

This observation inspired further modifications of the optical structure, as the back-side emission is considered to be lost for most applications. Demonstrated methods in the literature for circumventing such back-side emission include the employment of a large-area cathode[36] or the removal of the microlenses directly above the light-emission area.[33] The latter method has proven to be applicable when the light-emission area corresponded to the diameter of a few microlenses (i.e., on the order of 100 μm). Here, we choose to utilize a centimeter-sized large-area metallic reflector in the form of Al foil, which was glued onto the entire air-exposed area of the encapsulation glass; see Figure 1 for a schematic.

Figure 6c,d presents the temporal evolution of the voltage and luminance, respectively, during galvanostatic driving of a bare LEC (black solid squares), a LOF-attached LEC (red open circles), and an LEC with a LOF attached to the front side and metallic reflector laminated to the back side (blue crossed triangles). The voltage is independent of the modifications of the outer surfaces of the device structure, whereas the luminance is strongly affected. As discussed previously, the inclusion of the LOF increases the luminance by ∼40 %, whereas the combined inclusion of a LOF on the front side and a metallic reflector on the back side results in a luminance improvement of ∼60 % throughout the entire measurement period of 100 h. This improvement was verified by measurements on 27 independent devices.

Encouraged by the results in Figure 6, we also fabricated and characterized 10 different glass-encapsulated ITO/PEDOT-PSS/{Super Yellow:Trimethylolpropane ethoxylate:-$LiCF_3SO_3$}/Al LECs with included LOF and metallic reflector. We choose to include this active material into the study because it has shown superior (albeit more varying) performance compared to the {Super Yellow:PEO:KCF_3SO_3} active material.[18] We find a larger variation in performance for these devices than for the devices depicted in Figure 6, as exemplified by the peak PCE variation of between 10 and 15 lm W^{-1}; the cause for this lower reproducibility is currently not known. The champion device in this set exhibited a peak PCE of 15.6 lm W^{-1} at a luminance of 100 cd m^{-2}, and its optoelectronic performance during a 100 h measurement period is shown in Figure 7. This value represents a significant improvement in efficiency by >60% in comparison to the previous study on nominally similar devices with no light-outcoupling,[18] and it is also the highest reported PCE for a singlet-emitting LEC to our knowledge. It is worth emphasizing that this peak PCE value is recorded at a luminance level of practical interest.[54,60]

A common setback with large-area LECs is a non-homogenous luminance over the device surface, as visualized in the photograph of a 7.0 × 10.5 mm^2 ITO/PEDOT-PSS/{Super Yellow:PEO:KCF_3SO_3}/Al LEC in Figure 8a and the accompanying 3D plot of the light-emission intensity as a function of spatial position in Figure 8b. This problem can be attributed to a number of issues, including: (i) a phase separation between the different active-material constituents, (ii) an introduction of dust particles during device fabrication, and/or (iii) a spatial variation of the active-material thickness with a corresponding spatial variation in self-absorption.[61] These are all, to some extent, LEC-specific problems, as the technology benefits from the attractive opportunity of utilizing a fault-tolerant thick active material, commonly comprising a blend of a polar electrolyte and a nonpolar semiconductor, in a functional device that is fabricated under ambient (and therefore dusty) conditions.[8]

In this context, it was encouraging to observe that the problem of nonhomogenous light emission can be effectively suppressed by the introduction of the LOF. Figure 8c displays the emission from the same device as in Figure 8a after a LOF has been laminated onto its front-glass surface. In agreement with the observation in Figure 5c, we find that the emission edges became blurred with the introduction of the LOF. More importantly, however, is that the LOF inclusion results in a distinctly improved spatial uniformity of the light-emission over the entire device surface. This observation is quantified in the 3D plots of the light-emission intensity, which reveal an average-normalized standard deviation of σ_N = 3.8% for the bare LEC in Figure 8b and σ_N = 1.7% for the LOF-attached LEC in Figure 8d. We note that a light-uniformity improvement also has been reported for LOF-encapsulated small-area LEDs.[62,63]

4. CONCLUSIONS

The outcoupled light emission from a LEC can be improved by a factor of 1.6 by employing the straightforward and scalable procedure of laminating a LOF onto the front side of the device and a large-area metallic reflector onto the back side. It is important that this decisive improvement in device performance was attained without compromising the light-emission quality, as evidenced by the retension of both the Lambertian emission profile and the electroluminescence spectrum. The LOF, which comprised a hexagonal array of hemispherical microlenses as surface structure, randomized the outcoupled light-emission pattern with the additional positive effect that the problem of spatially nonhomogenous light emission in large-area LECs was mitigated.

AUTHOR INFORMATION

Corresponding Author

*Phone: +46-90-7865732; Fax: +46-90-7866673; E-mail: ludvig.edman@physics.umu.se.

Author Contributions

All authors have given approval to the final version of the manuscript.

Notes

The authors declare no competing financial interest.

ACKNOWLEDGMENTS

We acknowledge Vetenskapsrådet, Energimyndigheten, Kempestiftelserna, Carl Tryggeŕs Foundation, and Umeå University for financial support. L.E. is a Royal Swedish Academy of Sciences Research Fellow supported by a grant from the Knut and Alice Wallenberg Foundation.

REFERENCES

(1) Pei, Q.; Yu, G.; Zhang, C.; Yang, Y.; Heeger, A. J. Polymer Light-Emitting Electrochemical Cells. *Science* **1995**, *269*, 1086−1088.

(2) Pei, Q. B.; Yang, Y.; Yu, G.; Zhang, C.; Heeger, A. J. Polymer Light-Emitting Electrochemical Cells: In Situ Formation of a Light-Emitting p-n Junction. *J. Am. Chem. Soc.* **1996**, *118*, 3922−3929.

(3) Sun, Q. J.; Li, Y. F.; Pei, Q. B. Polymer Light-Emitting Electrochemical Cells for High-Efficiency Low-Voltage Electroluminescent Devices. *J. Disp. Technol.* **2007**, *3*, 211−224.

(4) Costa, R. D.; Orti, E.; Bolink, H. J.; Monti, F.; Accorsi, G.; Armaroli, N. Luminescent Ionic Transition-Metal Complexes for Light-Emitting Electrochemical Cells. *Angew. Chem., Int. Ed.* **2012**, *51*, 8178−8211.

(5) Fang, J. F.; Matyba, P.; Edman, L. The Design and Realization of Flexible, Long-Lived Light-Emitting Electrochemical Cells. *Adv. Funct. Mater.* **2009**, *19*, 2671−2676.

(6) van Reenen, S.; Kersten, S. P.; Wouters, S. H. W.; Cox, M.; Janssen, P.; Koopmans, B.; Bobbert, P. A.; Kemerink, M. Large Magnetic Field Effects in Electrochemically Doped Organic Light-Emitting Diodes. *Phys. Rev. B* **2013**, *88*, 125203.

(7) Tordera, D.; Bunzli, A. M.; Pertegas, A.; Junquera-Hernandez, J. M.; Constable, E. C.; Zampese, J. A.; Housecroft, C. E.; Orti, E.; Bolink, H. J. Efficient Green-Light-Emitting Electrochemical Cells Based on Ionic Iridium Complexes with Sulfone-Containing Cyclometalating Ligands. *Chem.—Eur. J.* **2013**, *19*, 8597−8609.

(8) Sandström, A.; Dam, H. F.; Krebs, F. C.; Edman, L. Ambient Fabrication of Flexible and Large-Area Organic Light-Emitting Devices Using Slot-Die Coating. *Nat. Commun.* **2012**, *3*, 1002-1−1002-5.

(9) Liang, J. J.; Li, L.; Niu, X. F.; Yu, Z. B.; Pei, Q. B. Fully Solution-Based Fabrication of Flexible Light-Emitting Device at Ambient Conditions. *J. Phys. Chem. C* **2013**, *117*, 16632−16639.

(10) Matyba, P.; Yamaguchi, H.; Eda, G.; Chhowalla, M.; Edman, L.; Robinson, N. D. Graphene and Mobile Ions: The Key to All-Plastic, Solution-Processed Light-Emitting Devices. *ACS Nano* **2010**, *4*, 637−642.

(11) Liang, J. J.; Li, L.; Niu, X. F.; Yu, Z. B.; Pei, Q. B. Elastomeric Polymer Light-Emitting Devices and Displays. *Nat. Photonics* **2013**, *7*, 817−824.

(12) Reineke, S.; Lindner, F.; Schwartz, G.; Seidler, N.; Walzer, K.; Lussem, B.; Leo, K. White Organic Light-Emitting Diodes with Fluorescent Tube Efficiency. *Nature* **2009**, *459*, 234−238.

(13) Mladenovski, S.; Neyts, K.; Pavicic, D.; Werner, A.; Rothe, C. Exceptionally Efficient Organic Light Emitting Devices Using High Refractive Index Substrates. *Opt. Express* **2009**, *17*, 7562−7570.

(14) Tanaka, D.; Sasabe, H.; Li, Y. J.; Su, S. J.; Takeda, T.; Kido, J. Ultra High Efficiency Green Organic Light-Emitting Devices. *Jpn. J. Appl. Phys., Part 2* **2007**, *46*, L10−L12.

(15) Helander, M. G.; Wang, Z. B.; Qiu, J.; Greiner, M. T.; Puzzo, D. P.; Liu, Z. W.; Lu, Z. H. Chlorinated Indium Tin Oxide Electrodes with High Work Function for Organic Device Compatibility. *Science* **2011**, *332*, 944−947.

(16) Bolink, H. J.; Coronado, E.; Costa, R. D.; Lardies, N.; Orti, E. Near-Quantitative Internal Quantum Efficiency in a Light-Emitting Electrochemical Cell. *Inorg. Chem.* **2008**, *47*, 9149−9151.

(17) Su, H. C.; Wu, C. C.; Fang, F. C.; Wong, K. T. Efficient Solid-State Host-Guest Light-Emitting Electrochemical Cells Based on Cationic Transition Metal Complexes. *Appl. Phys. Lett.* **2006**, *89*, 261118-1−261118-3.

(18) Tang, S.; Edman, L. Quest for an Appropriate Electrolyte for High-Performance Light-Emitting Electrochemical Cells. *J. Phys. Chem. Lett.* **2010**, *1*, 2727−2732.

(19) Yang, Y.; Pei, Q. B. Efficient Blue-Green and White Light-Emitting Electrochemical Cells Based on Poly[9,9-bis(3,6-dioxaheptyl)-fluorene-2,7-diyl]. *J. Appl. Phys.* **1997**, *81*, 3294−3298.

(20) Yu, Z. B.; Wang, M. L.; Lei, G. T.; Liu, J.; Li, L.; Pei, Q. B. Stabilizing the Dynamic p-i-n Junction in Polymer Light-Emitting Electrochemical Cells. *J. Phys. Chem. Lett.* **2011**, *2*, 367−372.

(21) Sun, Y. R.; Giebink, N. C.; Kanno, H.; Ma, B. W.; Thompson, M. E.; Forrest, S. R. Management of Singlet and Triplet Excitons for Efficient White Organic Light-Emitting Devices. *Nature* **2006**, *440*, 908−912.

(22) Cleave, V.; Yahioglu, G.; Le Barny, P.; Friend, R. H.; Tessler, N. Harvesting Singlet and Triplet Energy in Polymer LEDs. *Adv. Mater.* **1999**, *11*, 285−288.

(23) Friend, R. H.; Gymer, R. W.; Holmes, A. B.; Burroughes, J. H.; Marks, R. N.; Taliani, C.; Bradley, D. D. C.; Dos Santos, D. A.; Bredas, J. L.; Logdlund, M.; Salaneck, W. R. Electroluminescence in Conjugated Polymers. *Nature* **1999**, *397*, 121−128.

(24) Ho, P. K. H.; Kim, J. S.; Burroughes, J. H.; Becker, H.; Li, S. F. Y.; Brown, T. M.; Cacialli, F.; Friend, R. H. Molecular-Scale Interface Engineering for Polymer Light-Emitting Diodes. *Nature* **2000**, *404*, 481−484.

(25) Kohler, A.; Wilson, J. S.; Friend, R. H. Fluorescence and Phosphorescence in Organic Materials. *Adv. Mater.* **2002**, *14*, 701−707.

(26) Evans, N. R.; Devi, L. S.; Mak, C. S. K.; Watkins, S. E.; Pascu, S. I.; Kohler, A.; Friend, R. H.; Williams, C. K.; Holmes, A. B. Triplet Energy Back Transfer in Conjugated Polymers with Pendant Phosphorescent Iridium Complexes. *J. Am. Chem. Soc.* **2006**, *128*, 6647−6656.

(27) Kabra, D.; Lu, L. P.; Song, M. H.; Snaith, H. J.; Friend, R. H. Efficient Single-Layer Polymer Light-Emitting Diodes. *Adv. Mater.* **2010**, *22*, 3194−3198.

(28) Baldo, M. A.; O'Brien, D. F.; You, Y.; Shoustikov, A.; Sibley, S.; Thompson, M. E.; Forrest, S. R. Highly Efficient Phosphorescent Emission from Organic Electroluminescent Devices. *Nature* **1998**, *395*, 151−154.

(29) Baldo, M. A.; Thompson, M. E.; Forrest, S. R. High-Efficiency Fluorescent Organic Light-Emitting Devices Using a Phosphorescent Sensitizer. *Nature* **2000**, *403*, 750−753.

(30) Han, T. H.; Lee, Y.; Choi, M. R.; Woo, S. H.; Bae, S. H.; Hong, B. H.; Ahn, J. H.; Lee, T. W. Extremely Efficient Flexible Organic

Light-Emitting Diodes with Modified Graphene Anode. *Nat. Photonics* **2012**, *6*, 105−110.
(31) Uoyama, H.; Goushi, K.; Shizu, K.; Nomura, H.; Adachi, C. Highly Efficient Organic Light-Emitting Diodes from Delayed Fluorescence. *Nature* **2012**, *492*, 234−238.
(32) Moller, S.; Forrest, S. R. Improved Light Out-Coupling in Organic Light Emitting Diodes Employing Ordered Microlens Arrays. *J. Appl. Phys.* **2002**, *91*, 3324−3327.
(33) Lin, H. Y.; Ho, Y. H.; Lee, J. H.; Chen, K. Y.; Fang, J. H.; Hsu, S. C.; Wei, M. K.; Lin, H. Y.; Tsai, J. H.; Wu, T. C. Patterned Microlens Array for Efficiency Improvement of Small-Pixelated Organic Light-Emitting Devices. *Opt. Express* **2008**, *16*, 11044−11051.
(34) Lee, J. H.; Ho, Y. H.; Chen, K. Y.; Lin, H. Y.; Fang, J. H.; Hsu, S. C.; Lin, J. R.; Wei, M. K. Efficiency Improvement and Image Quality of Organic Light-Emitting Display by Attaching Cylindrical Microlens Arrays. *Opt. Express* **2008**, *16*, 21184−21190.
(35) Wei, M. K.; Lin, C. W.; Yang, C. C.; Kiang, Y. W.; Lee, J. H.; Lin, H. Y. Emission Characteristics of Organic Light-Emitting Diodes and Organic Thin-Films with Planar and Corrugated Structures. *Int. J. Mol. Sci.* **2010**, *11*, 1527−1545.
(36) Eom, S. H.; Wrzesniewski, E.; Xue, J. G. Close-Packed Hemispherical Microlens Arrays for Light Extraction Enhancement in Organic Light-Emitting Devices. *Org. Electron.* **2011**, *12*, 472−476.
(37) Sun, Y.; Forrest, S. R. Organic Light Emitting Devices with Enhanced Outcoupling via Microlenses Fabricated by Imprint Lithography. *J. Appl. Phys.* **2006**, *100*, 073106-1−073106-6.
(38) Madigan, C. F.; Lu, M. H.; Sturm, J. C. Improvement of Output Coupling Efficiency of Organic Light-Emitting Diodes by Backside Substrate Modification. *Appl. Phys. Lett.* **2000**, *76*, 1650−1652.
(39) Krummacher, B. C.; Mathai, M. K.; Choong, V.; Choulis, S. A.; So, F.; Winnacker, A. General Method to Evaluate Substrate Surface Modification Techniques for Light Extraction Enhancement of Organic Light Emitting Diodes. *J. Appl. Phys.* **2006**, *100*, 054702-1−054702-6.
(40) Chen, S. M.; Kwok, H. S. Light Extraction from Organic Light-Emitting Diodes for Lighting Applications by Sand-Blasting Substrates. *Opt. Express* **2010**, *18*, 37−42.
(41) Bathelt, R.; Buchhauser, D.; Garditz, C.; Paetzold, R.; Wellmann, P. Light Extraction from OLEDs for Lighting Applications Through Light Scattering. *Org. Electron.* **2007**, *8*, 293−299.
(42) Frischeisen, J.; Niu, Q. A.; Abdellah, A.; Kinzel, J. B.; Gehlhaar, R.; Scarpa, G.; Adachi, C.; Lugli, P.; Brutting, W. Light Extraction from Surface Plasmons and Waveguide Modes in an Organic Light-Emitting Layer by Nanoimprinted Gratings. *Opt. Express* **2011**, *19*, A7−A19.
(43) Geyer, U.; Hauss, J.; Riedel, B.; Gleiss, S.; Lemmer, U.; Gerken, M. Large-Scale Patterning of Indium Tin Oxide Electrodes for Guided Mode Extraction from Organic Light-Emitting Diodes. *J. Appl. Phys.* **2008**, *104*, 093111-1−093111-5.
(44) Matterson, B. J.; Lupton, J. M.; Safonov, A. F.; Salt, M. G.; Barnes, W. L.; Samuel, I. D. W. Increased Efficiency and Controlled Light Output from a Microstructured Light-Emitting Diode. *Adv. Mater.* **2001**, *13*, 123−127.
(45) Yamasaki, T.; Sumioka, K.; Tsutsui, T. Organic Light-Emitting Device with an Ordered Monolayer of Silica Microspheres as a Scattering Medium. *Appl. Phys. Lett.* **2000**, *76*, 1243−1245.
(46) Sandstrom, A.; Matyba, P.; Edman, L. Yellow-Green Light-Emitting Electrochemical Cells with Long Lifetime and High Efficiency. *Appl. Phys. Lett.* **2010**, *96*, 053303-1−053303-3.
(47) Shao, Y.; Bazan, G. C.; Heeger, A. J. Long-Lifetime Polymer Light-Emitting Electrochemical Cells. *Adv. Mater.* **2007**, *19*, 365−370.
(48) Shin, J. H.; Robinson, N. D.; Xiao, S.; Edman, L. Polymer Light-Emitting Electrochemical Cells: Doping Concentration, Emission-Zone Position, and Turn-On Time. *Adv. Funct. Mater.* **2007**, *17*, 1807−1813.
(49) Jhang, Y. P.; Chen, H. F.; Wu, H. B.; Yeh, Y. S.; Su, H. C.; Wong, K. T. Improving Device Efficiencies of Solid-State White Light-Emitting Electrochemical Cells by Adjusting the Emissive-Layer Thickness. *Org. Electron.* **2013**, *14*, 2424−2430.
(50) Hernandez-Sosa, G.; Eckstein, R.; Tekoglu, S.; Becker, T.; Mathies, F.; Lemmer, U.; Mechau, N. The Role of the Polymer Solid Electrolyte Molecular Weight in Light-Emitting Electrochemical Cells. *Org. Electron.* **2013**, *14*, 2223−2227.
(51) Li, X. Y.; Gao, J.; Liu, G. J. Thickness Dependent Device Characteristics of Sandwich Polymer Light-Emitting Electrochemical Cell. *Org. Electron.* **2013**, *14*, 1441−1446.
(52) Li, X. Y.; Gao, J.; Liu, G. J. Reversible Luminance Decay in Polymer Light-Emitting Electrochemical Cells. *Appl. Phys. Lett.* **2013**, *102*, 039904-1−039904-4.
(53) Asadpoordarvish, A.; Sandström, A.; Tang, S.; Granström, J.; Edman, L. Encapsulating Light-Emitting Electrochemical Cells for Improved Performance. *Appl. Phys. Lett.* **2012**, *100*, 193508-1−193508-4.
(54) Forrest, S. R.; Bradley, D. D. C.; Thompson, M. E. Measuring the Efficiency of Organic Light-Emitting Devices. *Adv. Mater.* **2003**, *15*, 1043−1048.
(55) Leger, J. M.; Carter, S. A.; Ruhstaller, B. Recombination Profiles in Poly[2-methoxy-5-(2-ethylhexyloxy)-1,4-phenylenevinylene] Light-Emitting Electrochemical Cells. *J. Appl. Phys.* **2005**, *98*, 124907-1−124907-7.
(56) Elschner, A.; Kirchmeyer, S.; Lövenich, W.; Merker, U.; Reuter, K. *PEDOT: Principles and Applications of an Intrinsically Conductive Polymer*; CRC Press: Boca Raton, FL, 2011; p 142.
(57) *TFD Product Data Pages*; Thin Film Devices Inc.: Anaheim, CA; http://tfdinc.com/transparent_conductors_detail.htm. (accessed October 15, 2013).
(58) *Corning EAGLE XG Glass Substrates Material Information Page*; Corning Inc.: Corning, NY; http://www.corning.com/WorkArea/showcontent.aspx?id=55075 (accessed October 15, 2013).
(59) Kim, J. S.; Ho, P. K. H.; Greenham, N. C.; Friend, R. H. Electroluminescence Emission Pattern of Organic Light-Emitting Diodes: Implications for Device Efficiency Calculations. *J. Appl. Phys.* **2000**, *88*, 1073−1081.
(60) Tordera, D.; Frey, J.; Vonlanthen, D.; Constable, E.; Pertegás, A.; Orti, E.; Bolink, H. J.; Baranoff, E.; Nazeeruddin, M. K. Low Current Density Driving Leads to Efficient, Bright, and Stable Green Electroluminescence. *Adv. Energy Mater.* **2013**, *3*, 1338−1343.
(61) Kaihovirta, N.; Asaadpoordarvish, A.; Sandström, A.; Edman, L. Doping-Induced Self-Absorption in Light-Emitting Electrochemical Cells. *ACS Photonics*, Accepted for publication.
(62) Lee, H. W.; Lin, B. S. Improvement of Illumination Uniformity for LED Flat Panel Light by Using Micro-Secondary Lens Array. *Opt. Express* **2012**, *20*, A788−A798.
(63) Huang, C. Y.; Hsiao, W. T.; Huang, K. C.; Chang, K. S.; Chou, H. Y.; Chou, C. P. Fabrication of a Double-Sided Micro-lens Array by a Glass Molding Technique. *J. Micromech. Microeng.* **2011**, *21*, 085020.